Journal of the European Ceramic Society 23 (2003) 409–416

www.elsevier.com/locate/jeurceramsoc

Universal hardness and elastic recovery in Vickers nanoindentation of copper phosphate and silicate glasses

T. Miura[a], Y. Benino[a], R. Sato[b], T. Komatsu[a,*]

[a]*Department of Chemistry, Nagaoka University of Technology, Nagaoka 940-2188, Japan*
[b]*Department of Materials Engineering, Tsuruoka National College of Technology, Tsuruoka 997-8511, Japan*

Received 28 December 2001; received in revised form 12 April 2002; accepted 28 April 2002

Abstract

Load/unload displacement (penetration) curves for $y\mathrm{CuO}_x\cdot(100-y)\mathrm{P_2O_5}$ glasses ($y=45$, 50) with different copper valence states, silica and soda-lime silicate glasses at room temperature (humidity ~64%) have been measured using a Vickers nanoindentation technique, and universal hardness H_u and elastic recovery E_R have been estimated in the load range of 0.1–1 N. Copper phosphate glasses have the values of $H_u=1.7$–2.5 GPa and $E_R=0.55$–0.65, depending on the Cu^+/Cu^{2+} ratio. The glasses with high Cu^+ contents show large densifications (plastic deformation) during loading and small elastic recoveries during unloading compared with the glasses with no Cu^+ ions. These deformation behaviors are well explained qualitatively by considering lower coordination number and more covalent bonding of Cu^+ compared with Cu^{2+}, which have been confirmed from X-ray photoelecton spectra. Silica glass has $E_R\fallingdotseq0.77$, which is large compared with $E_R\fallingdotseq0.63$ in a soda-lime silicate glass. This large difference leads to the smaller value in H_u of silica glass than that of a soda-lime silica glass. It is confirmed that load displacement curves in nanoindentation tests are well fitted with quadratic equations.

Keywords: Copper phosphate; Glass; Hardness; Nanoindentation; Silicate

1. Introduction

When a sharp indenter such as Vickers indenter is loaded onto a glass, a residual surface impression is observed after unloading, and the material hardness is conveniently estimated from the projected area of the impression. It is known that some extent of deformation during loading is recovered during unloading, i.e., elastic recovery.[1,2] Since it is expected that the degree of elastic recovery depends on glass systems and glass compositions, the hardness evaluated from a residual surface impression after unloading is insufficient for an in-depth understanding of deformation behaviors in glass. In this point of view, it is also important to evaluate the hardness during loading, i.e., the so-called "universal hardness". So far, numerous studies of mechanical and elastic properties of glasses such as Vickers hardness and Young's modulus have been carried out, but reports on the elastic recovery of glasses and universal hardness are small.[1–7] On the other hand, irreversible (non-recoverable) deformation in indentation tests has been regarded as plastic (shear) deformation, which is divided into two deformation components: densification and plastic flow.[8–10] Therefore, in order to understand the deformation mechanism in glass, it is necessary to clarify contributions of densification and plastic flow to plastic deformation.

Glasses containing copper have various attractive points such as high-T_c superconducting precursors, semiconducting, superionic conducting, very low thermal expansion, laser and optical nonlinear glasses. Copper can exist in glasses as cuprous Cu^+ or cupric Cu^{2+} ions, and it is known that the valence state in copper affects not only chemical/physical properties but also the glass-forming ability.[11,12] Very recently, the present authors' group found that CuO–P_2O_5 glasses show extremely unusual elastic and mechanical properties depending on the Cu^+/Cu^{2+} ratio.[13] Particularly, some glasses with high Cu^+/Cu^{2+} ratios have a large fracture toughness of $K_c\fallingdotseq1.1$ MPam$^{1/2}$, indicating a high resistance against crack formation in Vickers indentation tests. They proposed that the unusual elastic and mechanical properties

* Corresponding author. Tel.: +81-258-47-9313; fax: +81-258-47-9300.
E-mail address: komatsu@chem.nagaokaut.ac.jp (T. Komatsu).

0955-2219/02/$ - see front matter
PII: S0955-2219(02)00154-1

of copper phosphate glasses are explained qualitatively by considering unique oxygen coordination and bonding states of Cu^+ ions, i.e., lower coordination number and more covalent bonding compared with Cu^{2+} ions. It is of particular interest to examine universal hardness, elastic recovery and plastic deformation and to clarify the deformation mechanism in copper phosphate glasses more in detail. Furthermore, it is desired to clarify the bonding state of Cu^+ ions in copper phosphate glasses and to demonstrate the structure and bonding role of Cu^+ ions proposed in the previous papers.[12,13]

In the present study, firstly the chemical bonding state of Cu^+ ions in $yCuO_x\cdot(100-y)P_2O_5$ glasses ($y=45$, 50) with different copper valence states, i.e., $R(Cu^+)=Cu^+/(Cu^+ + Cu^{2+})$, was clarified from X-ray photoelectron spectroscopy (XPS), and then universal hardness, elastic recovery and plastic deformation were examined by a Vickers nanoindentation technique. To the best of our knowledge, the data on universal hardness and elastic recovery of silica and soda-lime silicate glasses which are most important and standard glasses are also insufficient, and therefore nanoindentation experiments were carried out for those glasses in this study. The deformation mechanism in copper phosphate glasses was compared with those of silica and soda-lime silicate glasses. Such information will lead to designs of less-brittle glasses.

2. Experimental procedure

The nominal compositions examined in the present study are $yCuO_x\cdot(100-y)P_2O_5$ ($y=45$, 50). A mixture of reagent grades of CuO and H_3PO_4 was reacted and dried at 200 °C for 2 h and melted in an alumina crucible at 1200 °C for 30 min in an electric furnace. The batch weight was 20 g. The melts were poured onto an iron plate and pressed quickly to a thickness of 1–2 mm. The glasses were ground, and glucose (1–4 wt.%) was added to control the copper valence state. The mixture was remelted in a covered alumina crucible at 1200 °C for 10 min in an electric furnace. The melts were cast on an iron plate heated to 150 °C. The bulk glasses were annealed at temperatures of T_g+10 K for 15 min to release internal stress. Glass transition temperatures, T_g, were determined by using differential thermal analysis (DTA) at a heating rate of 10 K/min. Cu^+ contents in the glasses, i.e. $R(Cu^+)=Cu^+/(Cu^+ + Cu^{2+})$, were analyzed by cerate titration within an accuracy of $\pm 5\%$.[12] Fused silica glass was obtained from Asahi Glass company, and a soda-lime silicate glass ($\sim 12.7Na_2O\cdot 5.9MgO\cdot 9.4CaO\cdot 0.9Al_2O_3\cdot 71.0SiO_2$ mol%) was obtained from Nippon Sheet Glass company.

XPS measurements were carried out using a SHIMADZU ESCA-3200 electron spectrometer which has Al conical anode for charge control. Non-monochromatic 240 W Mg-K_α X-ray provided the excitation radiation. During experiments the pressure inside the analyzer chamber was $\sim 10^{-7}$ Pa. XPS spectra of O1s (oxygen) core level of fresh glass surfaces were recorded. Drift of the electron binding energy due to surface charging effect was calibrated by utilizing the C1s (carbon) peak of the contamination of the pumping oil at sample introduction chamber ($E_B=284.6$ eV).

Universal hardness during loading and the fraction of elastic recovery after unloading were evaluated from load/unload displacement curves obtained using a nanoindentation apparatus (Akashi, MZT-4). Measurements were carried out at room temperature in air (relative humidity was ~64%). Fig. 1 shows a schematic load/unload displacement curve for a nonflat indenter with definitions of load P, indentation depth h, the peak indentation load P_{max}, the indenter displacement at peak load h_t, and the final depth of the contact impression after unloading h_f. In this study, a Vickers indenter was used. The load and unload speed was 49 mN/s and the maximum load was ~980 mN. Within this maximum load, any crack is not observed during Vickers indentations.[13] The displacement (penetration depth) during loading gives universal hardness, H_u, which is expressed by the following equation.

$$H_u = \frac{P_{max}}{26.43h_t^2} \quad (1)$$

The elastic recovery, E_R, corresponds to the area ratio in the indentation hysteresis loop, i.e., the ratio of the recovered area (h_f-A-h_t) and the total area ($0-A-h_t$). Since the product of load P (N) and displacement h (m) has a dimension of energy (J), the elastic recovery means the fraction of the consumed energy for elastic deformation to the consumed energy for total (elastic + plastic) deformation.

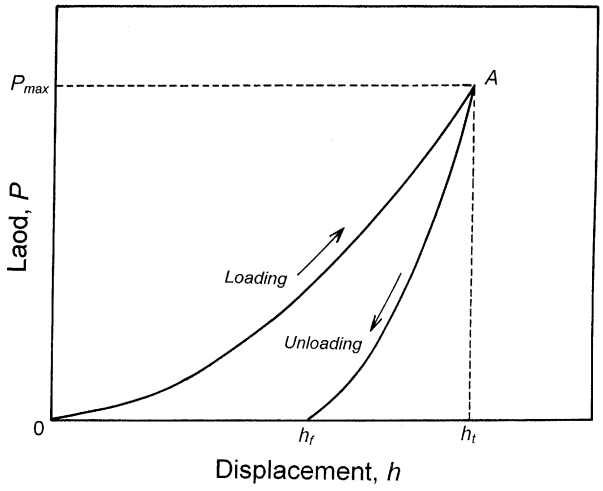

Fig. 1. A schematic load/unload displacement curve in a nonflat indentation experiment for elastoplastic materials. P_{max}, h_t, h_f are the peak indentation load, the indenter displacement at peak load, and the final depth of the contact impression after unloading, respectively.

Table 1
Values of copper valence ratio $R(Cu^+)=Cu^+/(Cu^+ + Cu^{2+})$, glass transition temperature T_g, density d, mean atomic volume V_m, usual Vickers hardness H_v, Young's modulus E, and fracture toughness K_c for $yCuO_x\cdot(100-y)P_2O_5$ glasses

Glass	$R(Cu^+)$ ±0.03	T_g (°C) ±2	d (g/cm^3) ±0.01	V_m (cm^3/g-atom) ±0.02	H_v (GPa) ±0.1	E (GPa) ±0.1	K_c (MPa.m$^{1/2}$)
$y=45$	0.00	431	3.21	7.46	4.3	66.8	0.92±0.04
	0.57	218	3.17	7.63	2.7	50.6	0.91±0.06
$y=50$	0.00	431	3.32	7.41	4.4	72.9	0.72±0.04
	0.43	279	3.28	7.56	3.4	60.4	1.14±0.05

The values of H_v, E, and K_c are taken from our previous paper.[13]

3. Results

The values of T_g and $R(Cu^+)=Cu^+/(Cu^+ + Cu^{2+})$ for copper phosphate glasses examined in the present study are summarized in Table 1, in which the values of mean atomic volume, Young's modulus E, Vickere hardness H_v, and fracture toughness K_c reported in the previous paper [13] are also given. As reported by Sato et al.,[12] the change in chemical compositions during the melting for glass preparation is very small and the contamination of alumina from the crucible is about 1 mol%, irrespective of the amount of glucose. It was confirmed from infrared (IR) spectroscopy that some amounts of OH groups are present in all glasses prepared in the present study. Although quantitative analyses have not been conducted, the intensity of the absorption peaks at around 3000 cm^{-1} due to OH groups is not so strong.

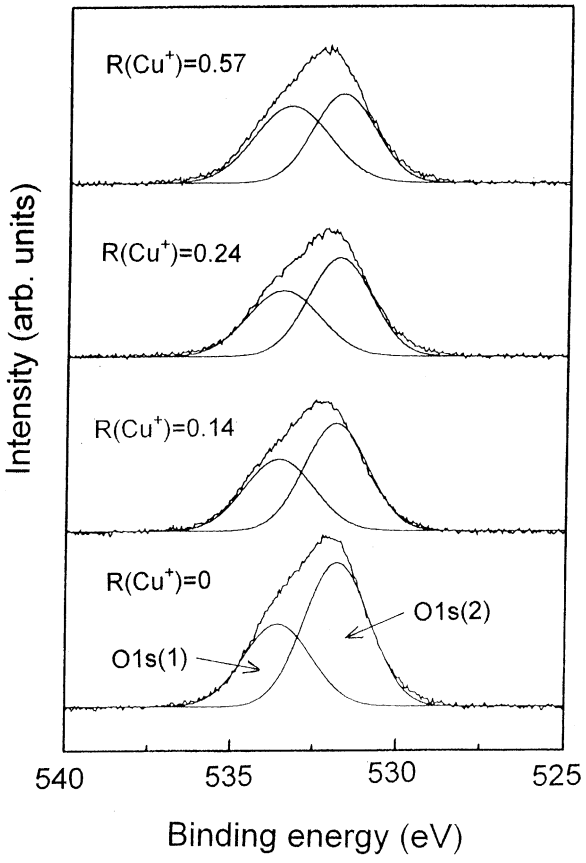

Fig. 2. Oxygen 1s photoelectron spectra at room temperature for $45CuO_x\cdot55P_2O_5$ glasses with different copper valence states, $R(Cu^+)=Cu^+/(Cu^+ + Cu^{2+})$.

3.1. Bonding state of Cu^+ in copper phosphate glasses

The XPS spectra near the O1s levels obtained for $45CuO_x\cdot55P_2O_5$ glasses are shown in Fig. 2. Similar XPS spectra were obtained for $50CuO_x\cdot50P_2O_5$ glasses. It is observed that the O1s spectra have asymmetric peaks. The spectra shown in Fig. 2 were fitted to decompose the asymmetric peaks by a sum of Gaussian curves by means of least square method with a linear background subtraction. As shown in Fig. 2, the oxygen 1s (O1s) signal in the spectra of $45CuO_x\cdot55P_2O_5$ glasses can be decomposed into two components denoted in the text as O1s(1) and O1s(2) with a good fitting quality. The maximum peaks are observed at ~534 eV for O1s(1) and at ~532 eV for O1s(2). The fraction of O1s(1) peak intensity in the O1s spectra is plotted as a function of $R(Cu^+)$ in Fig. 3, showing almost a linear correlation between them.

XPS spectra for some alkali phosphate and zinc phosphate glasses have been reported, and it has been well analyzed that the high binding energy peak near 534 eV is related to bridging oxygens that link neighboring phosphorus atoms in PO_4 tetrahedra and the low binding energy peak near 532 eV corresponds to non-bridging oxygens and oxygens with double bonds, giving a quantitative measure of the ratio of bridging and non-bridging oxygens.[14–16] XPS studies for copper phosphate and sodium copper phosphate glasses have been reported, but the valence state of copper ions in those glasses are unclear.[17,18]

By assuming that Cu^{2+} ions in copper phosphate glasses create only non-bridging oxygens and on the other hand Cu^+ ions create only bridging oxygens, the fraction of bridging oxygens in copper phosphate glasses was calculated as a function of $R(Cu^+)$. The results are shown in Fig. 3. It is seen that the data on the fraction of O1s(1) peak intensity estimated from XPS spectra lie well on the calculated lines (solid lines in Fig. 3).

The XPS spectra shown in Fig. 2, therefore, support the structure and bonding model for the role of copper ions in copper phosphate glasses proposed in the previous papers.[12,13] That is, Cu^+ ions in copper phosphate glasses are surrounded by two oxygen atoms through covalent bond and bridge two phosphate chains. The structural and bonding roles of Cu^+ and Cu^{2+} ions in copper phosphate glasses are completely different.

3.2. Universal hardness and elastic recovery

The load/unload displacement curves at various maximum loads for $50CuO_x{\cdot}50P_2O_5$ glass with $R(Cu^+)=0.43$ are shown in Fig. 4 as a typical example. Similar load/unload displacement curves were obtained for other copper phosphate, silica and soda-lime silicate glasses. The values of universal hardness H_u and elastic recovery E_R estimated from the load/unload displacement curves for copper phosphate, silica, soda-lime silicate glasses are shown in Figs. 5 and 6 as a function of P_{max}, respectively. The following features are obtained. In copper phosphate glasses, the H_u values are 1.7–2.5 GPa and increase slightly with decreasing load. $50CuO_x{\cdot}50P_2O_5$ glasses have higher H_u values compared with $45CuO_x{\cdot}55P_2O_5$ glasses. The glasses with $R(Cu^+)=0.43$ and 0.57 have slightly large H_u values compared with the glasses with $R(Cu^+)=0$. The E_R values are 0.55–0.65 and decrease gradually with decreasing load. The elastic recovery depends strongly on the Cu^+/Cu^{2+} ratio. That is, the E_R values in the glasses with $R(Cu^+)=0.43$ and 0.57 are much smaller than those in the glasses with $R(Cu^+)=0$. In silica and soda-lime silicate glasses, the H_u values depend strongly on the load, and silica glass has smaller H_u values compared with a soda-lime silicate glass. Silica glass has the E_R values of $\sim$0.77, which are larger than the E_R values of $\sim$0.63 in a soda-lime silicate glass. These results demonstrate that the universal hardness and elastic recovery are very sensitive to glass systems and compositions.

As shown in Fig. 5, the universal hardness increases with decreasing load. This phenomenon is known as

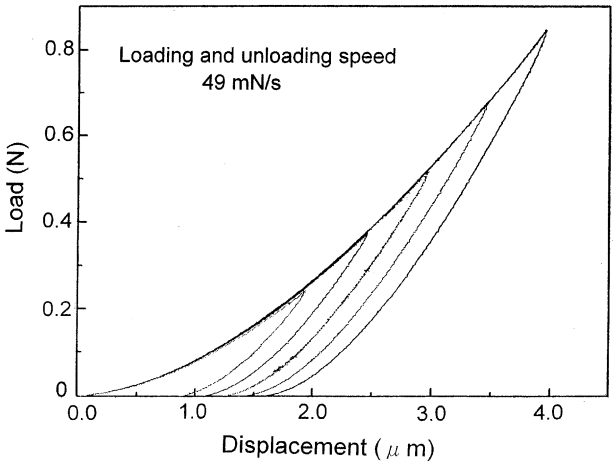

Fig. 4. Load/unload displacement curves at room temperature in air for $50CuO_x{\cdot}50P_2O_5$ glass with $R(Cu^+)=0.43$. The load and unload speed was 49 mN/s.

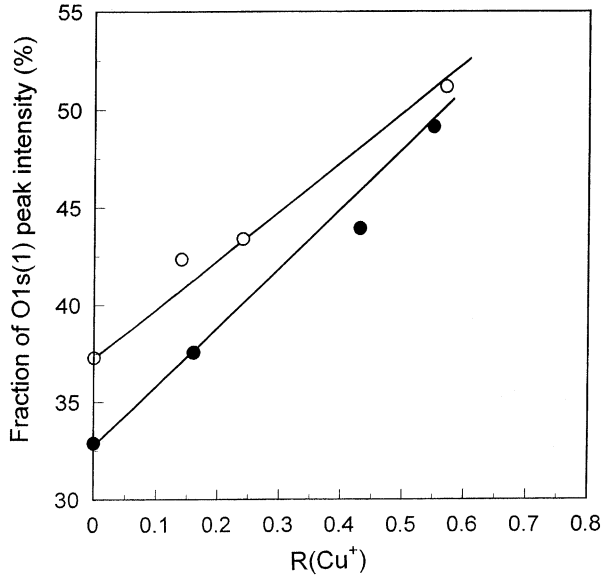

Fig. 3. Fractions of O1s(1) component in oxygen 1s photoelectron spectra for $yCuO_x{\cdot}(100-y)P_2O_5$ glasses with $y=45$ and 50 as a function of copper valence states, $R(Cu^+)=Cu^+/(Cu^++Cu^{2+})$. The solid lines represent the fraction of bridging oxygens calculated by assuming that Cu^{2+} ions create only non-bridging oxygens and Cu^+ ions create only bridging oxygens. ○: $y=45$, ●: $y=50$.

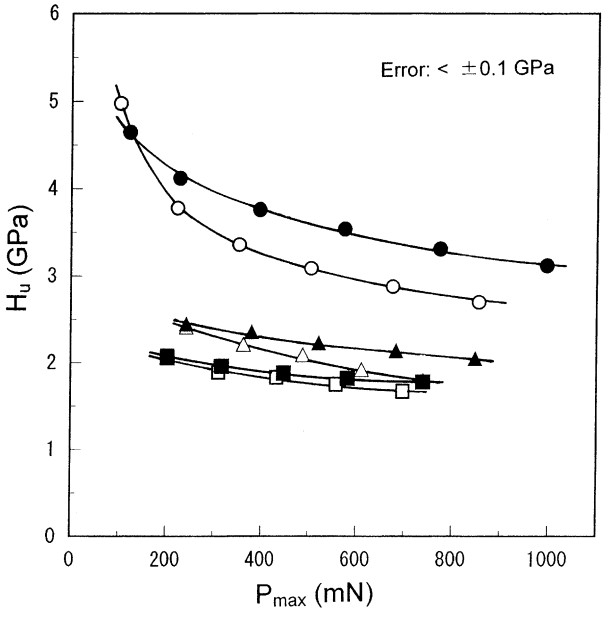

Fig. 5. Correlation between the maximum load P_{max} and universal hardness H_u for copper phosphate, silica and soda-lime silicate glasses. ○: silica, ●: soda-lime silicate, □: $45CuO_x{\cdot}55P_2O_5$ with $R(Cu^+)=0$, ■: $45CuO_x{\cdot}55P_2O_5$ with $R(Cu^+)=0.57$, △: $50CuO_x{\cdot}50P_2O_5$ with $R(Cu^+)=0$, ▲: $50CuO_x{\cdot}50P_2O_5$ with $R(Cu^+)=0.43$.

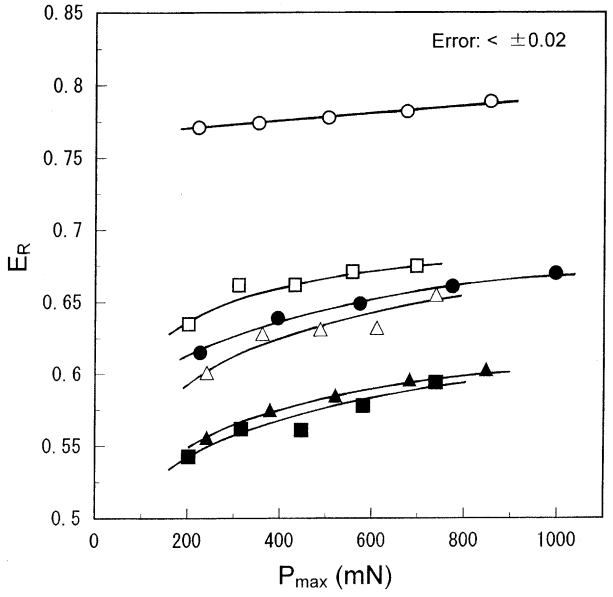

Fig. 6. Correlation between the maximum load P_{max} and elastic recovery E_R for copper phosphate, silica and soda-lime silicate glasses. ○: silica, ●: soda-lime silicate, □: $45CuO_x{\cdot}55P_2O_5$ with $R(Cu^+)=0$, ■: $45CuO_x{\cdot}55P_2O_5$ with $R(Cu^+)=0.57$, △: $50CuO_x{\cdot}50P_2O_5$ with $R(Cu^+)=0$, ▲: $50CuO_x{\cdot}50P_2O_5$ with $R(Cu^+)=0.43$.

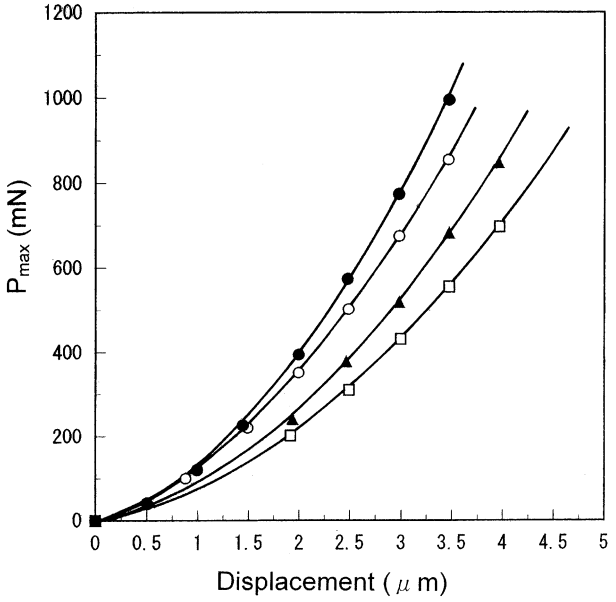

Fig. 7. Correlation between displacement depth h_t and the maximum load P_{max} for copper phosphate, silica and soda-lime silicate glasses. ○: silica, ●: soda-lime silicate, □: $45CuO_x{\cdot}55P_2O_5$ with $R(Cu^+)=0$, ▲: $50CuO_x{\cdot}50P_2O_5$ with $R(Cu^+)=0.43$.

indentation size effect (ISE).[19–21] The microscopic mechanism for ISE is still open to discussion,[19–21] and in this paper we do not touch deeply the ISE in our samples. It should be, however, pointed out that the ISE in copper phosphate glasses in the load range of 0.1–1 N is weak compared with silica and soda-lime silicate glasses.

Since the load versus displacement curve during loading corresponds to the consumed energy for the total deformation, it seems to be very important to express the curve using a mathematical function. It was found that all load versus displacement curves in the load range of 0.1–1 N for copper phosphate, silica and soda-lime silicate glasses can be well fitted by quadratic equations, $P=Ah^2+Bh+C$, where A, B, C are the constant. Since the universal hardness and elastic recovery of these glasses depend on load as shown in Figs. 5 and 6, it is clear that load versus displacement curves are not expressed by simple quadratic equations of $P=Ah^2$. Some typical data are shown in Fig. 7, in which the experimental data and the fitting curves are given. The parameters of A, B and C in the fitting quadratic equations are summarized in Table 2. It is noted that the parameter C is small compared with the parameters A and B, but is not zero. It was confirmed that at least these parameters are constants for the different loading speeds of 19.6, 49, and 98 mN/s. The results shown in Fig. 7 demonstrate again that the copper phosphate glasses can deform with small energies compared with silica and soda-lime silicate glasses.

Table 2
Values of the parameters in well-fitted quadratic equations, $P=Ah^2+Bh+C$, for load displacement curves obtained by Vickers nanoindentation tests at room temperature in air, where P is the load and h is the displacement depth

Glass	A(mN/μm^2)	B(mN/μm)	C(mN)
SiO_2	48.48	82.31	−5.70
Soda-lime silicate	61.34	78.94	−9.34
$45CuO_x{\cdot}55P_2O_5$			
$R(Cu^+)=0$	34.18	40.85	−0.45
$R(Cu^+)=0.57$	39.71	29.58	−0.28
$50CuO_x{\cdot}50P_2O_5$			
$R(Cu^+)=0$	29.57	72.69	−1.87
$R(Cu^+)=0.43$	42.30	48.45	−1.39

The loading speed was 49 mN/s, and the load range is 0.1–1 N.

3.3. Densification in plastic deformation

The plastic deformation at far below glass transition temperature includes densification and plastic flow.[8,9] Densification has been considered to be a more close-packed arrangement of atoms without breaking molecular bonds.[8,9] A portion of the densification is recoverable by annealing at relatively low temperatures below T_g.[8] On the other hand, plastic flow occurred during loading in indentation tests is an irreversible phenomenon and is caused by shear stress, probably through breaking of chemical bonds.

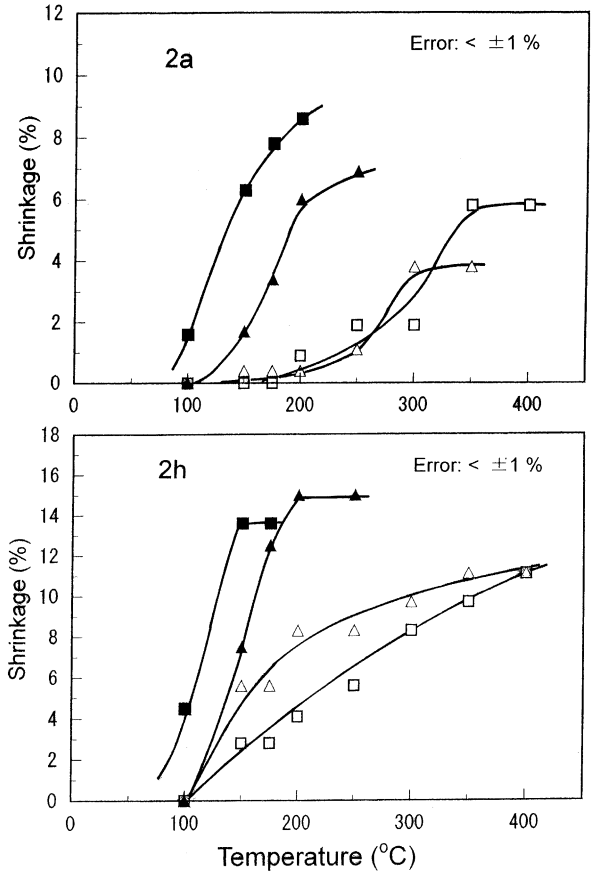

Fig. 8. Fraction of the shrinkages for the diagonal, 2*a*, and for the distance between counter edges, 2*h*, in the Vickers impressions as a function of annealing temperature for copper phosphate glasses. The precursor impressions before annealing were obtained by Vickers indentations with a load of 294 mN. □: $45CuO_x{\cdot}55P_2O_5$ with $R(Cu^+)=0$, ■: $45CuO_x{\cdot}55P_2O_5$ with $R(Cu^+)=0.57$, △: $50CuO_x{\cdot}50P_2O_5$ with $R(Cu^+)=0$, ▲: $50CuO_x{\cdot}50P_2O_5$ with $R(Cu^+)=0.43$.

Considering the above deformation model in glass, it is very important to clarify the shape change in a residual indentation impression by annealing after unloading. The data in copper phosphate glasses are shown in Fig. 8, in which the fraction of the shrinkages for the diagonal, 2*a*, and for the distance between counter edges, 2*h*, in the Vickers impressions are plotted as a function of annealing temperature. The size of the impressions was measured from scanning electron microscope observations. The precursor impressions before annealing were obtained by Vickers indentations with a load of 294 mN. It is seen that the distinct shrinkages in both 2*a* and 2*h* are observed in all glasses. It is clear that such shrinkages are observed by annealing at temperatures well below T_g, demonstrating that densifications which are recovered by annealing occur in copper phosphate glasses as similar to silica and soda-lime silicate glasses.[8,22] Furthermore, it is noted that the fraction of the shrinkage in 2*h* is much large compared with that in 2*a*. It should be pointed out that the shrinkages in the copper phosphate glasses with $R(Cu^+)=0.43$ and 0.57 are larger than those in the glasses with $R(Cu^+)=0$. These results indicate that the copper phosphate glasses with high Cu^+ contents have a large amount of densification compared with the glasses with low Cu^+ contents.

4. Discussion

4.1. Silica and soda-lime silicate glasses

It is well known that the structure of silica glass having no non-bridging oxygens is not compact, but very open, and the strength of Si–O bonds is strong, giving the high glass transition temperature, T_g, of around 1200 °C. It is, therefore, considered that atoms or structural units (SiO_4) can move without bond breaking even in the condition of relatively large applied loads, but by changing the angle of Si–O–Si bonds during loading. Indeed, a distinct densification (i.e. plastic deformation) has been observed during loading in Vickers indentations of silica glass.[8–10] It is also expected that a structural change during loading recovers largely during unloading due to strong Si–O–Si bonds. This would be the reason for a small universal hardness (in Fig. 5) and a large elastic recovery of around 77% (in Fig. 6) in silica glass. On the other hand, in a soda-lime silicate glass showing around $T_g=550$ °C, a large amount of modifiers (Na_2O and CaO) are included, leading to the formation of non-bridging oxygens and weaker bonds such as Na^+–O. It is, therefore, considered that the structure of soda-lime silicate glass is more compact compared with silica glass. Such structural and bonding features would cause a large permanent deformation, i.e., a small elastic recovery. Indeed, genuine plastic (shear) flow has been observed under indenter loading in soda-lime silicate glasses.[10] As seen in Fig. 5, the universal hardness of silica glass, i.e., the degree of total (elastic + plastic) deformation during loading, is small compared with a soda-lime silicate glass. This demonstrates that silica glass can deform largely during loading. As reported by Kurkjian,[9] however, silica glass has larger Vickers hardness ($H_v=7$ GPa at room temperature) compared with a soda-lime silicate glass ($H_v=5.5$ GPa). It is obvious that such a difference in the usual Vickers hardness arises from a large difference in the elastic recovery in these glasses.

4.2. Copper phosphate glasses

Combined with the results on the elastic recovery (Fig. 6) and the densification (Fig. 7), it is obvious that the plastic deformation is more easily induced during loading in the copper phosphate glasses with high Cu^+ contents. It is also clear that such a strong tendency to

the plastic deformation due to densification is closely related to the more open glass structure due to the low coordination number of Cu^+ ions.

The coordination and bonding states of copper ions in copper phosphate glasses are largely different, as demonstrated from XPS measurements in the present study. It is suggested that Cu^{2+} ions having an ionic bonding character act as modifier ions, leading to the formation of non-bridging oxygens, but Cu^+ ions having a covalent bonding character are surrounded by two oxygen atoms and bridge two phosphate chains. The two oxygen coordination state of Cu^+ has been also proposed in other copper containing glasses such as $Cu_2O{\cdot}Al_2O_3{\cdot}4SiO_2$ and $Bi_2Sr_2CaCu_2O_x$ glasses.[23,24] The structure of $50CuO_x{\cdot}50P_2O_5$ glass with $R(Cu^+)=0.43$ is, therefore, considered to be more open compared with the glass with $R(Cu^+)=0$. From these structural features, it is expected that copper phosphate glasses with high Cu^+ contents show larger elastic recovery than the glasses with low Cu^+ contents, as similar to silica glass. But, the data in Fig. 5 indicate an opposite trend. As seen in Table 1, the glass transition temperature of $50CuO_x{\cdot}50P_2O_5$ glass with $R(Cu^+)=0.43$, $T_g=279$ °C, is much smaller than that ($T_g=431$ °C) of the glass with $R(Cu^+)=0$. And, it is considered that the introduction of Cu^+ ions changes the network structure from a three-dimension to a two-dimension. This bonding state in copper phosphate glasses seems to be completely different compared with silica glass, although the copper phosphate glasses with high Cu^+ contents show large densifications during Vickers indenter loading as similar to silica glass. This would be the reason that the elastic deformation during indenter loading in copper phosphate glasses decreases with increasing Cu^+/Cu^{2+} ratio. It should be also pointed out that the large densification (plastic deformation) in the glasses with high Cu^+ contents leads to the decrease in the elastic recovery. In the previous paper,[13] it was found that the fracture toughness of the copper phosphate glasses increases with increasing Cu^+/Cu^{2+} ratio. It is concluded from the present study that a strain energy given by a Vickers indenter is consumed through movements of constituent atoms toward open spaces without bond breaking, i.e., through densification. Sato et al.[12] proposed that the single bond strength of Cu^+-O is stronger than that of Cu^{2+}–O, and as shown in Fig. 1, the mean oxygen 1s binding energy increases with increasing Cu^+/Cu^{2+} ratio. This difference might be related to the small difference in the universal hardness shown in Fig. 5.

Phosphate glasses with high transparency for ultraviolet light are becoming important in optical technology, and their structure and physical/chemical properties have been investigated extensively so far.[25] Recently, Kurkjian [26] and Karabulut et al.[27] have studied the mechanical properties of some phosphate glass fibers. To the best of our knowledge, however, there has been no report on universal hardness and elastic recovery of phosphate glasses except our present study. It is strongly desired to study the correlation between structure and universal hardness/elastic recovery in other phosphate glasses, and such information will lead to designs for glasses with high fracture toughness.

5. Conclusion

As described in the introduction, information on universal hardness and elastic recovery of glasses, even for silicate glasses, is lacking compared with the study of other properties such as physical and optical properties. In this study, load/unload displacement curves for $yCuO_x{\cdot}(100-y)P_2O_5$ glasses ($y=45$, 50) with different copper valence states, silica and soda-lime silicate glasses at room temperature (humidity ~64%) were measured by using a Vickers nanoindentation technique, and universal hardness H_u and elastic recovery E_R were estimated in the load range of 0.1–1 N. Copper phosphate glasses have the values of $H_u=1.7$–2.5 GPa and $E_R=0.55$–0.65, depending on the Cu^+/Cu^{2+} ratio. The glasses with high Cu^+ contents show large densification (plastic deformation) during loading and small elastic recovery during unloading compared with the glasses with no Cu^+ ions. These deformation behaviors are well explained qualitatively by considering lower coordination number and more covalent bonding of Cu^+ compared with Cu^{2+}, which were confirmed from XPS spectra. These results support our previous model [13] on unusual elastic and mechanical behaviors of copper phosphate glasses. The E_R values of silica glass are around 0.77 and those of soda-lime silicate glass are around 0.63, leading to the smaller H_u values in silica glass compared with a soda-lime silica glass.

Acknowledgements

This work was supported by the Grant-in-Aid for Scientific Research of the Ministry of Education, Sports and Culture in Japan.

References

1. Lawn, B. R. and Howes, V. R., Elastic recovery at hardness indentations. *J. Mater. Sci.*, 1981, **16**, 2745–2752.
2. Oliver, W. C. and Pharr, G. M., An improved technique for determining hardness and elastic modulus using load and displacement sensing indentation experiments. *J. Mater. Res.*, 1992, **7**, 1564–1583.
3. Michels, B. D. and Frischat, G. H., Microhardness of chalcogenide glasses of the system Se–Ge–As. *J. Mater. Sci.*, 1982, **17**, 329–334.
4. Frischat, G. H., Őzmen, E., Richter, T. and Michels, B. D., Load-independent microhardness of various glasses. *Glastech. Ber.*, 1982, **55**, 119–125.

5. Grau, P., Berg, G., Fränzel, W. and Schinker, M., Load dependence of the hardness of silica glasses—not just due to indenter tip defects. *Glastech. Ber.*, 1993, **66**, 313–320.
6. Watanabe, T., Muratsubaki, K., Benino, Y., Saitoh, H. and Komatsu, T., Hardness and elastic properties of Bi_2O_3-based glasses. *J. Mater. Sci.*, 2001, **36**, 2427–2434.
7. Torres, F., Benino, Y., Komatsu, T. and Lavelle, C., Mechanical and elastic properties of transparent nanocrystalline TeO_2-based glass-ceramics. *J. Mater. Sci.*, 2001, **36**, 4961–4968.
8. Neely, J. E. and Mackenzie, J. D., Hardness and low-temperautre deformation of silica glass. *J. Mater. Sci.*, 1968, **3**, 603–609.
9. Peter, K. W., Densification and flow phenomena of glass in indentation experiments. *J. Non-Cryst. Solids*, 1970, **5**, 103–115.
10. Kurkjian, C. R., Kammlott, G. W. and Chaudhri, M. M., Indentation behavior of soda-lime silica Glass, fused silica, and single-crystal quartz at nitrogen temperature. *J. Am. Ceram. Soc.*, 1995, **78**, 737–744.
11. Bae, B. S. and Weinberg, M. C., Chemical durability of copper phosphate glasses. *Glass Technol.*, 1994, **35**, 83–88.
12. Sato, R., Komatsu, T. and Matusita, K., Unique physical properties and fragility of $50CuO_x$–$50P_2O_5$ glasses. *J. Non-Cryst. Solids*, 1996, **201**, 222–230.
13. Miura, T., Watanabe, T., Benino, Y. and Komatsu, T., Unusual elastic and mechanical behaviors of copper phosphate glasses with different copper valence States. *J. Am. Ceram. Soc.*, 2001, **84**, 2401–2408.
14. Gresch, R., Warmuth, W. M. and Dutz, H., X-ray photoelectron spectroscopy of sodium phosphate glasses. *J. Non-Cryst. Solids*, 1979, **34**, 127–136.
15. Onyiriuka, E. C., Zinc phosphate glass surfaces studies by XPS. *J. Non-Cryst. Solids*, 1993, **163**, 268–273.
16. Brow, R. K., An XPS study of oxygen bonding in zinc phosphate and zinc borophosphate glasses. *J. Non-Cryst. Solids*, 1996, **194**, 267–273.
17. Salim, M. A., Khattak, G. D. and Hussain, M. S., X-ray photoelectron spectroscopy, fourier transform infrared spectroscopy and electrical conductivity studies of copper phosphate glasses. *J. Non-Cryst. Solids*, 1995, **185**, 101–108.
18. Shih, P. Y., Yung, S. W. and Chin, T. S., FTIR and XPS studies of P_2O_5–Na_2O–CuO glasses. *J. Non-Cryst. Solids*, 1999, **244**, 211–222.
19. Hirao, K. and Tomozawa, M., Microhardness of SiO_2 glass in various environments. *J. Am. Ceram. Soc.*, 1987, **70**, 497–502.
20. Li, H. and Bradt, R. C., The indentation load/size effect and the measurement of the hardness of vireous silica. *J. Non-Cryst. Solids*, 1992, **146**, 197–212.
21. Nix, W. D. and Gao, H., Indentation size effects in crystalline materials: a law for strain gradient plasticity. *J. Mech. Phys. Solids*, 1998, **46**, 411–425.
22. Yoshida, S., Isono, S., Matsuoka, J. and Soga, N., Shrinkage behavior of Knoop indentations in silica and soda-lime-silica glasses. *J. Am. Ceram. Soc.*, 2001, **84**, 2141–2143.
23. Kamiya, K., Okasaka, K., Wada, M., Nasu, H. and Yoko, T., EXAFS study on the local environment around copper in low thermal expansion copper aluminosilicate glasses. *J. Am. Ceram. Soc.*, 1992, **75**, 477–478.
24. Nakagawa, Z., Morikawa, H., Sung, T. H., Yoshimura, M., Marumo, F. and Udagawa, Y., EXAFS study of coordination of Cu atom in amorphous $Bi_2Sr_2CaCu_2O_x$. *Nippon Kagaku Kaishi*, 1989, **110**, 2085–2087.
25. Brow, R. K., Review: the structure of simple phosphate glasses. *J. Non-Cryst. Solids*, 2000, **263&264**, 1–28.
26. Kurkjian, C. R., Mechanical properties of phosphate glasses. *J. Non-Cryst. Solids*, 2000, **263&264**, 207–212.
27. Karabulut, M., Melnik, E., Stefan, R., Marasinghe, G. K., Ray, C. S., Kurkjian, C. R. and Day, D. E., Mechanical and structural properties of phosphate glasses. *J. Non-Cryst. Solids*, 2001, **288**, 8–17.